Serine/threonine kinase TBK1 promotes Intrahepatic cholangiocarcinoma progression via direct regulation of β-catenin

Chongqing Gao
School of Medicine, Jinan University
Zhenzhen Chu
School of Medicine
Yang Xiao
Jinan University
Xingyan Zhou
Jinan University
Junru Wu
Jinan University
Hui Yuan
Huizhou Municipal Central Hospital
Yuchuan Jiang
the First Affiliated Hospital, Jinan University
Dong Chen
the First Affiliated Hospital Sun Yat sen University
Ji-chun Zhang
Jinan University https://orcid.org/0000-0001-6035-6867
Nan Yao
School of Medicine, Jinan University
Kaiyun Chen
Guangdong Second Provincial General Hospital
JIAN HONG (hongjian7@jnu.edu.cn)
Jinan University

Article

Keywords: TBK1, Intrahepatic cholangiocarcinoma (ICC), EMT, β-Catenin, progression

Posted Date: July 5th, 2022

DOI: https://doi.org/10.21203/rs.3.rs-1774135/v1

Abstract

Intrahepatic Cholangiocarcinoma (ICC) is an aggressive liver bile duct malignancy with limited therapeutic options. Metastasis is one of the main contributors to ICC progression and poor prognosis. However, the underlying mechanism of ICC metastasis remains largely unknown. Here, we showed that TANK-binding kinase 1 (TBK1), a serine/threonine-protein kinase, was significantly upregulated in tumor tissues of ICC patients with larger tumor diameter, lymph node metastasis, and advanced TNM stage. Consistently, during the different stages of Cholangiocarcinoma (CCA) carcinogenesis (hyperplasia, dysplasia, and CCA), TBK1 showed a dynamic increase in spontaneous rat and mouse models. Functional studies showed that enforced expression of TBK1 promoted metastasis both in vitro and in vivo. Mechanistically, TBK1 directly interacts with β-catenin and stimulates its nuclear translocation, further activating the β-catenin-mediated epithelial-mesenchymal transition (EMT) process. Moreover, we demonstrate that the S172 site of TBK1 kinase domain was essential for the interaction between TBK1 and β-catenin as well as for TBK1 mediated β-catenin activation. In addition, high levels of TBK1 in clinical ICC tissues were correlated with elevated nuclear β-catenin levels and predicted worse overall and disease-free survival. A TBK1 inhibitor GSK-8612 and the liver-specific accumulation of DNA/RNA heteroduplex oligonucleotide (TBK1-HDO) significantly reduced TBK1 expression of ICC and inhibited its intrahepatic metastasis. In summary, our study demonstrated that TBK1 could activate β-catenin via protein-protein interaction, then promote EMT and ICC metastasis, which might serve as a potential therapeutic target for patients with cholangiocarcinoma.

Introduction

Cholangiocarcinoma (CCA), the second most common primary cancer of the liver, is a highly malignant epithelial neoplasm with cholangiocyte differentiation [1, 2]. According to anatomical location, CCAs are classified as intrahepatic (ICC) and extrahepatic Cholangiocarcinoma (ECC) [3]. In the past decade, a progressive increase in ICC incidence worldwide while the incidences of ECC seem to be decreasing [4]. Although radical resection and systemic chemotherapy have shown remarkable improvements [5, 6], the prognosis of patients with ICC remains dismal due to malignant proliferation and metastasis [7, 8]. The development of targeted therapies that address disease pathogenesis or progression has lagged because of the complex and unclear pathogenesis [9]. Therefore, there is an urgent need to investigate the molecular mechanisms underlying ICC metastasis to develop potential therapeutic strategies to target ICC metastasis.

Epithelial-mesenchymal transition (EMT) plays a vital role in the induction of tumor cell invasion and metastasis [10]. EMT has been reported to promote tumor progression and metastasis in pancreatic ductal adenocarcinoma (PDAC) [6, 11]. ICC shares anatomic, embryologic, and genetic features with PDAC [12, 13]. However, the functions of EMT in ICC have not been studied thoroughly *in vivo*. EMT involves a cellular reprogramming process that drives epithelial cells into a mesenchymal-like phenotype, characterized by the loss of epithelial surface markers like E-cadherin and the acquisition of the mesenchymal markers vimentin and N-cadherin [14, 15]. Thus, EMT has been recognized as a

prometastatic cellular event that promotes tumor cell invasion and malignant tumor progression [16, 17]. Recent studies have shown that a series of transcription factors are direct repressors of E-cadherin, including β-catenin, a dual-function protein implicated in transcriptional regulation and cell-cell adhesion [18]. In normal epithelial cells, most β-catenin forms an adhesion complex with E-cadherin and is located in cell-cell adherent junctions at the membrane. In tumor cells, β-catenin detaches from the complex, and activation by nuclear translocation promotes the EMT process, further repressing E-cadherin expression [19]. Nevertheless, the molecular mechanisms by which β-catenin translocates into the nucleus remain largely unknown.

Tumor necrosis factor (TNF) receptor-associated factor (TRAF) family member-associated NF-κB activator TANK-Binding Kinase 1 (TBK1), which is also known as NAK, T2K, is a serine/threonine-protein kinase that plays essential roles in cancer development and progression [20, 21]. TBK1 has been demonstrated to contribute to tumorigenicity in human pancreatic cancer by promoting cell growth, migration, and invasion [11, 22]. Despite the growing interest in studying the roles and regulation of TBK1 in cancer, the precise molecular mechanisms governing TBK1 signaling and its subsequent impact on cancer biology remain incompletely understood.

This study found that TBK1 was upregulated in ICC and correlated with ICC metastasis. Enforced expression of TBK1 stimulated the metastatic potential of CCA cells via induction of the EMT process. In addition, we revealed that TBK1 direct interacted with and activated β-catenin and promoted its nuclear translocation. Moreover, we showed a positive correlation between TBK1 and the nuclear expression of β-catenin. Pharmacological inhibition of TBK1 by GSK-8612 and TBK1-HDO effectively suppressed ICC intrahepatic metastasis. Taken together, our data indicate that the overexpression of TBK1 promotes ICC metastasis through β-catenin-mediated induction of EMT and that TBK1 has the potential to be a prognostic factor and therapeutic target of ICC.

Results

TBK1 is upregulated in CCA

To clarify the underlying role of TBK1 in ICC, Tumor Immune Estimation Resource was used to analyze the transcriptome sequencing data from the TCGA data set. The results revealed that TBK1 expression was up-regulated in nine types of cancer, including ICC. (Fig. 1A, and Supplementary. Fig. 1A), suggesting that TBK1 may participate in the tumorigenesis and progression of several solid tumors. In addition, upregulated expression of TBK1 in ICC was confirmed by tissue microarray (cohort 1, n=91, Outdo Biotech, Shanghai, China) ($P < 0.001$; Fig. 1B, C). Next, we examined TBK1 expression status in hepatic tissues obtained from patients. IHC analysis showed a high level of cytosol-localized TBK1 in 76.4% (139/182) of the ICC and 85.0% (34/40) of the ECC compared to the non-tumor tissues ($P < 0.001$; Fig. 1D, E, and Supplementary. Fig. 1B, C). Similar results were also observed in the immunoblot analyses (Fig. 1F). Besides, RT-qPCR and western blot found that the expression of TBK1 was significantly higher in several ICC cell lines than in human normal bile duct HiBEPIC cells (Fig. 1G). Consistently, the TBK1

expression was dynamically upregulated during the different stages of CCA carcinogenesis (hyperplasia, dysplasia, and CCA) in Spontaneous ICC models induced by rats and mice (Supplementary. Fig. 2A, B). Supplementary Fig. 1D, E revealed that TBK1 was primarily expressed in ICC tissues. Then far, we examined the expression levels of TBK1 in the same patient's liver tissue by immunofluorescence staining. Our results showed that TBK1 expression was higher in the bile ducts with ICC, lower in the adjacent bile ducts with tumor invasion, and no TBK1 expression was detected from adjacent non-tumor tissues (including the left hepatic duct, interlobular bile duct, and capillary bile duct) (Fig. 1H).

High expression of TBK1 was associated with aggressive clinicopathological characteristics

To further investigate the clinical significance of TBK1 expression in ICC, all 182 ICC patients were divided into two groups based on the overall expression level of TBK1; the high TBK1 expression group (n = 139) and the low TBK1 expression group (n = 43). As shown in Supplementary Table 1, the upregulation of TBK1 was significantly correlated with several aggressive clinicopathological characteristics, such as high serum CEA ($P < 0.001$) and CA199 ($P = 0.008$), larger tumor diameter ($P = 0.009$), lymph node metastasis ($P < 0.001$), and advanced TNM stage ($P = 0.001$) (Fig. 2A). The correlation between TBK1 and tumor size, lymph node metastasis, or TNM stages suggested that TBK1 may be involved in tumor progression in ICC (Fig. 2B-D).

Upregulation of TBK1 promotes ICC cell growth, motility, and metastasis both *in vitro* and *in vivo*.

To elucidate the functions of TBK1 in ICC progression, we knocked out TBK1 in HuCCT1 cells, which exhibited relatively high endogenous TBK1 levels. In addition, we overexpressed TBK1 in TFK1 cells, which exhibited relatively low endogenous TBK1 levels (Fig. 3A). The CCK8 assay, wound healing migration, transwell migration, and matrigel invasion assays revealed that the overexpression of TBK1 enhanced the growth migration and invasion ability, vice versa. (Fig. 3B and Supplementary. Fig. 3A, B). Similarly, knockdown of TBK1 by specific siRNAs repressed cell growth, migration, and invasion in TBK1 highly expressed HuCCT1 and RBE cells (Supplementary Fig. 4 A-D).

Subsequently, a mouse subcutaneous xenograft model was developed to evaluate the effect of TBK1 on ICC progression *in vivo*. The tumor growth curve and tumor weight showed that tumors from TBK1 overexpression cells grew significantly faster (Figure 3C-E). Subsequently, we assessed Ki-67 expression by immunohistochemistry and found more positive cells in xenografts from TBK1 overexpression cells (Supplementary Fig. 5 A). These results were further validated in human ICC tissues (Supplementary Fig. 5 B). Furthermore, the orthotopic ICC model was established to determine whether TBK1 had the same effect on ICC metastasis *in vivo*. As shown in Fig. 3F, depletion of TBK1 significantly inhibited liver colonization of HuCCT1 cells, whereas overexpression of TBK1 significantly promoted liver colonization of TFK1 cells. Next, the cells mentioned above were used to establish a lung metastasis mouse model by tail vein injection. More metastatic nodules were observed in mice injected with TBK1 overexpression cells (Fig. 3G). These results indicate that TBK1 can promote the growth, invasion, and metastasis of ICC cells both *in vitro* and *in vivo*.

Upregulation of TBK1 promoted EMT in ICC cells

To further explore the potential mechanism of TBK1 in promoting tumor progression, we performed RNA-sequencing and detected approximately 3101 differentially expressed genes (DEGs) after TBK1 knockdown (Fig. 4A). The gene rank of these differential genes indicated that epithelial-associated genes were significantly upregulated, while mesenchymal-associated genes were downregulated. (Fig. 4B). Moreover, Gene Ontology (GO) enrichment analysis and Gene Set Enrichment Analysis (GSEA) revealed that the TBK1 knockdown regulated genes associated with several EMT-related signaling pathways, such as the Wnt signaling pathway and the β-catenin nucleic translocation pathway (Figure.4C, D). These data suggested that TBK1knockdown affected EMT remarkably in CCA cells.

Next, the mRNA expression levels of E-cadherin and a series of EMT inducers, including Vimentin, ZEB1, Snail, and Twist1, were measured in both TBK1-overexpressing and TBK1 knockdown cells. Overexpression of TBK1 stimulates the EMT process (Fig. 4E). Western blot analysis also confirmed the above results (Fig. 4F). We then assessed the clinical relationship between TBK1 and EMT in ICC tissues. Immunohistochemical staining displayed that ICC patients with low TBK1 expression showed higher E-cadherin and lowered Vimentin expression levels than ICC patients with high TBK1 expression (Fig. 4G). Moreover, correlation analyses showed that the expression of TBK1 correlated with the expression of E-cadherin (r = -0.3799,P ≤ 0.001) and Vimentin (r = 0.3818, P ≤ 0.001). Taken together, these results demonstrated that TBK1 plays a vital role in EMT in ICC (Fig. 4H).

TBK1 promotes the EMT process through β-catenin activation

β-Catenin plays a critical role in the induction of EMT during ICC metastasis [23]. To determine whether β-catenin is involved in the TBK1-mediated EMT process, we assessed the clinical relationship between TBK1 and β-catenin in ICC tissues. IHC showed that ICC patients with low TBK1 expression displayed lower nuclear β-catenin expression levels than ICC patients with high TBK1 expression (Fig. 5A). Consistent with this finding, correlation analyses showed that the protein expression of TBK1 was closely associated with that of nuclear β-catenin (r = 0.4807, P < 0.001) (Fig. 5B). These results suggested that TBK1 might promote the nuclear translocation of β-catenin.

Similar to the above findings, β-catenin was localized primarily in the cytoplasm of cells, which have relatively low levels of TBK1 expression. However, nuclear β-catenin was significantly enhanced in cells, showing relatively high levels of TBK1 expression (Fig. 5C). In addition, the cytosolic and nuclear fractions of cell lysates were separated to verify this finding. Neither overexpression nor knockdown of TBK1 significantly affected the total β-catenin level. However, TBK1 overexpression decreased the cytosolic β-catenin and increased the level of nuclear β-catenin, while the knockdown of TBK1 showed the opposite effect (Fig. 5D).

To determine whether the activation of β-catenin is essential for the TBK1-mediated promotion of EMT, XAV939 [24] was used to inhibit nuclear entry of β-catenin in TBK1-overexpressing cells and observed that inhibited nuclear entry of β-catenin eliminated the TBK1-mediated upregulation of Vimentin, as well

as the downregulation of E-cadherin (Fig. 5E). In line with this finding, the EMT-mediated upregulation of cell invasion and migration was abolished by β-catenin inhibited (Fig. 5F, G), suggesting that β-catenin plays a pivotal role in the TBK1-induced EMT process.

To further confirm the role of TBK1 in the EMT process, TGFβ1 was used to induce EMT in ICC cells [25]. As shown in Supplementary Fig. 6A, treatment with TGFβ1 promoted the nuclear translocation of β-catenin, elevated the transcriptional activity of β-catenin, decreased the expression of E-cadherin, and increased the levels of Vimentin, indicating that EMT was induced by TGFβ1 treatment. However, TGFβ1-induced EMT was significantly attenuated by inhibition of TBK1 (Supplementary Fig. 6A, B). Similarly, we found that inhibition of TBK1 abrogated the increase in cell motility induced by TGFβ1 (Supplementary Fig.6C, D). These results demonstrated that TBK1 overexpression leads to β-catenin activation, promoting the EMT process.

TBK1 activated β-catenin through direct interaction

The phosphorylate β-catenin at S552 has been demonstrated to promote β-catenin activation and nuclear translocation [26]. As we know, various kinases are activated, leading to the phosphorylation and activation of transcription factors. Thus, we hypothesize that TBK1, a serine/threonine-protein kinase, would stimulate β-catenin activation. To explore the mechanism of TBK1 promoting β-catenin activation, we first examined the specific S552 phosphorylation of β-catenin by immunoblot analyses. The levels of S552 phosphorylation were significantly reduced in HuCCT1-shTBK1 cells, and the opposite results were obtained in TBK1-overexpressing TFK1 cells, suggesting that TBK1 contributes to β-catenin activation via phosphorylation of S552 (Fig. 6A). The experimental findings are confirmed by molecular simulations (Fig. 6B). The interactions were further validated by immunoprecipitation with a TBK1 antibody (Fig 6C, D). Altogether, these findings identify that TBK1 overexpression stimulated the nuclear translocation and activation of β-catenin through direct interaction.

As shown in Fig. 6E, F, we constructed a TBK1 mutant in S172 and found the mutation eliminated the interaction between TBK1 and β-catenin and the nuclear translocation of β-catenin. Similarly, the TBK1-S172A mutant did not induce the EMT process and cell motility (Fig. 6I and Supplementary Fig. 8A, B).

We further confirm that GSK-8612 (2.0 μM), a TBK1 S172 specific inhibitor (Supplementary Fig.7A), did not affect proliferation but effectively inhibited TBK1 phosphorylation at S172 and increased E-cadherin and decreased Vimentin expression in both HuCCT1 and TFK1 cells (Fig. 6G, H and Supplementary Fig. 7B). Immunofluorescence analysis shows that GSK-8612 notably inhibits the nucleic expression of β-catenin in indicated cells (Supplementary Fig. 7C). Taken together, these results demonstrated that the active site of TBK1 is crucial for TBK1-mediated β-catenin activation.

TBK1-HDO and Pharmacological inhibition of TBK1 reduce CCA cells growth both *in vitro* and *in vivo*

Given that depletion of TBK1 by shRNA and siRNA inhibited human CCA cell growth, we further evaluated the effect of TBK1 inhibitors in our system. Here, we designed TBK1-HDO, a short DNA/RNA heteroduplex

oligonucleotide (Fig. 7A). Notably, the HDO carried cholesterol leading to ASO accumulation in the liver and was more potent at reducing the expression of TBK1 mRNA in the liver [27, 28] (Fig. 7B). Immunofluorescence staining shows the nucleic accumulation after treated TBK1-HDO at 0 min, 30 min, 60 min, and 90 min (Fig. 7C). AS shown in Fig. 7D, 7E, theTBK1-HDO significantly decreased TBK1 protein expression in indicated cells in a dose-dependent way. A relatively selective accumulation of fluorescence-labeled TBK1-HDO in the liver and other mice organs was detected by histological analysis (Fig. 7F) and quantifying the signal intensities (Fig. 7G). Furthermore, the orthotopic ICC model was established to determine whether TBK1 inhibitor had the same effect on ICC metastasis *in vivo*. As shown in Fig. 7H and 7I, GSK-8612 and TBK1-HDO remarkably inhibited liver colonization of HuCCT1 cells. Besides, GSK-8612 significantly inhibited the subcutaneous xenograft growth, which showed the same effection as gemcitabine, the first-line treatment for ICC. (Supplementary Fig. 9A-D). Taken together, these findings indicate that pharmacological inhibition of TBK1 decreases CCA cell growth both in *vitro* and *in vivo*.

Upregulation of TBK1 predicts poor survival in ICC patients

The prognostic implication of TBK1 in ICC was explored next. Kaplan–Meier survival analysis revealed that patients with a high level of TBK1 expression exhibited a significantly poorer overall survival (hazard ratio (HR), 3.78; 95% confidence interval (CI), 2.48–5.75) and disease-free survival (hazard ratio (HR), 2.97; 95% confidence interval (CI), 2.11–4.16) in our cohorts (Fig. 8A). Similar results were observed in cohort 1 (Supplementary. Fig. 10C). Unfortunately, it has no significance in TCGA and might be related to the small sample size. (Supplementary. Fig. 10A, B).

Consistently, nuclear β-catenin overexpression exhibited a significantly poorer overall survival and disease-free survival (Fig. 8B). Interestingly, we found that patients with low expression of both TBK1 and nuclear β-catenin had the best prognosis (Fig. 8C). Subsequently, TBK1 expression status and prognostic clinicopathological parameters identified by univariate analysis ($P < 0.01$) were entered into a multivariate model to identify independent predictors of overall survival. We found that TBK1 upregulation was an independent statistically significant risk factor for overall survival ($P < 0.001$, Fig. 8D), suggesting that upregulation of TBK1 may play a pivotal role in the overall survival of ICC patients. Taken together, these results indicated that the combination of TBK1 and nuclear β-catenin could serve as a biomarker in ICC for evaluating the metastatic potential and predicting the prognosis of ICC patients.

Discussion

Local and systemic metastasis is a major cause leading to a dismal prognosis of Intrahepatic Cholangiocarcinoma (ICC) [29, 30]. Evidence indicates that the β-catenin-mediated epithelial-mesenchymal transition (EMT) process plays a vital role in cancer metastasis but has been defined as an undruggable target [31, 32]. This study found that TBK1, a novel regulator upstream of β-catenin, activates β-catenin via protein-protein interaction, then promotes EMT and ICC metastasis (Fig. 9A). In contrast, inhibiting the expression of TBK1 exhibits the opposite effects. Moreover, we demonstrated that

TBK1 plays a vital role in mediating intrahepatic metastasis and lung colonization of CCA cells in mouse models.

Recent studies have demonstrated that TBK1 plays a vital role in cancer development and progression [33, 34]. TBK1 is a serine/threonine-protein kinase that participates in the post-transcriptional regulation of specific genes [6]. Previous studies have confirmed the distinct role of TBK1 in certain types of cancers, including pancreatic cancer, hepatocellular carcinoma, and breast carcinoma [35]. Under hypoxic conditions, TBK1 was hyperactivated (increased pSer172) and increased its stability, thereby promoting cancer cell growth [11]. Our previous study demonstrated that high TBK1 expression enhanced ICC invasion and predicted poor prognosis in patients with ICC [21]. However, the role of TBK1 has not been reported in ICC, which shares anatomic, embryologic, and genetic features with PDAC [12]. In the present study, we found that higher TBK1 expression in ICC exerts a critical role in maintaining the tumor-promoting function, indicating TBK1 is also a potential therapeutic target for ICC.

In recent years, it has become increasingly clear that EMT plays an essential role in cancer metastasis [36]. However, the most recent advances in EMT research have questioned the requirement for EMT in tumor metastasis. In one study, primary pancreatic ductal adenocarcinoma (PDAC) mouse models showed that EMT suppression does not alter PDAC metastasis [37]. Our study demonstrated that TBK1 upregulated induced the β-catenin-mediated EMT process. Since we proved that TBK1 promoted the migration and invasion of CCA cells, we hypothesized that TBK1 might stimulate ICC metastasis by promoting EMT. To exclude the possibility that EMT is dispensable for TBK1-induced ICC metastasis, we utilized a specific inhibitor targeting β-catenin, a key transcription factor involved in EMT, and concluded that EMT was required for TBK1-induced ICC metastasis. β-Catenin, as a critical factor in the Wnt/β-catenin pathway, is an essential transcriptional coactivator regulating EMT in cancers. It has been widely reported that the Wnt/β-catenin pathway plays a crucial role in cholangiocarcinoma tumorigenesis and metastasis [38]. In addition, our evidence has indicated that β-catenin is overexpressed in ICC tissues (characterized by increased nuclear expression in cancer cells) and promotes EMT of CCA cells. Together, we further verified that TBK1 promotes EMT by increasing the nuclear expression of β-catenin.

To our knowledge, the present study describes a novel mechanism by which TBK1 promotes EMT in cancer. We demonstrated that TBK1 activated the Wnt/β-catenin pathway. Although TBK1 did not enhance the total expression levels of β-catenin, it promoted the nuclear translocation of β-catenin, thereby stimulating the transcription of β-catenin downstream genes. TBK1 is located in the cytoplasm and functions via protein-protein interactions. Interestingly, β-catenin was also present in the cytoplasm, suggesting that TBK1 might promote the nuclear translocation of β-catenin through direct protein-protein interaction. To verify this hypothesis, we confirmed the interaction between TBK1 and β-catenin by immunoprecipitation and molecular docking simulation. Collectively, the results of our study linked TBK1 with β-catenin, thus clarifying the underlying mechanism of TBK1-mediated ICC metastasis. However, the detailed mechanisms by which the interaction between TBK1 and β-catenin promotes the nuclear translocation of β-catenin require further investigation.

Gemcitabine combined with cisplatin has long been a first-line treatment for presenting with unresectable or metastatic ICC patients, whereas drug resistance causes poor effectiveness [39, 40]. Although targeted therapies have revolutionized cancer treatment, no effective target molecule has been discovered for ICC. Therefore, new biomarkers and therapeutic targets for ICC are urgently needed. This study found that TBK1 inhibitors GSK-8612, a specific inhibitor for blocking TBK1 S172 phosphorylation, had significant antitumor activity. Our data show that GSK-8612 significantly reduced the growth, motility, and metastasis of CCA cells both *in vitro* and *in vivo*. Nucleic acid-based therapeutics represent a promising technology platform to manipulate gene targets. Previously reported a new nucleic acid drug named cholesterol conjugated DNA/RNA heteroduplex oligonucleotide (HDO) [27]. The HDO carried cholesterol leading to ASO accumulation in the liver and was more potent at reducing the expression of target mRNA in the liver. The HDO technology improved the efficacy of microRNA-targeted therapeutic oligonucleotides [41]. Here, we designed a TBK1-HDO leading to TBK1-ASO accumulation in the liver and was more efficient in reducing the expression of TBK1 mRNA in the liver. Similarly, we found that TBK1-HDO decreased the number of ICC tumors in the orthotopic ICC model. Our ligand-conjugated DNA/RNA heteroduplex opens a new horizon for human gene therapy as a novel class of oligonucleotide drugs.

Our study demonstrated that TBK1 promotes the EMT process by binding to β-catenin and increasing its nuclear expression in ICC. Knockout TBK1 expression abrogated the tumor-promoting effect and inhibited ICC progression. Overexpression of TBK1 and β-catenin in ICC is a strong indicator of high tumor aggressiveness and correlates with poor clinical outcomes. In conclusion, we identified that TBK1 plays a vital role in ICC metastasis and could be a potential prognostic biomarker and therapeutic target for ICC.

Materials And Methods

Human Samples

We analyzed the features of ICC with a tissue microarray that included 91 patients (OUTDO Biotech, Shanghai, China) and a cohort including 182 patients who had undergone curative liver resection at The First Affiliated Hospital Sun Yat-sen University between January 2015 and December 2020. In addition, 44 normal hepatic tissues obtained from patients who underwent resection due to benign hepatic lesions were used as normal controls. Another 40 ECC specimens were collected from the First Affiliated Hospital of Jinan University. All experiments involving human tissues were approved by the research and ethics committee of Jinan University, and informed consent was obtained from each patient.

In vivo models

For the mouse subcutaneous xenograft model, 2×10^6 cells were injected subcutaneously in the flank of nude mice (BALB/c, 6 weeks of age, n = 7 per group). After 4 weeks, mice were sacrificed, and the subcutaneous tumors were excised, imaged, and embedded in paraffin [42]. Lung metastasis model, 2×10^6 cells were injected into nude mice through the tail vein (BALB/c, 6 weeks of age, n = 7 per group). After 4 weeks, mice were sacrificed, and the lungs were excised, imaged, and embedded in paraffin [43].

The orthotopic mouse model of ICC was established as described previously. Briefly, mice were anesthetized, and 2×10^6 cells were injected into the subcapsular region of the middle lobe. After 4 weeks, mice were sacrificed, and the livers were excised, imaged, and embedded in paraffin. Tumor metastases were confirmed by hematoxylin and eosin staining.

All rats and mice were purchased from Guangdong Medical Laboratory Animal Center. The Institutional Animal Ethical Committee, Experimental Animal Center of Jinan University, reviewed and approved the experimental animal protocol, followed by the Guide for the Care and Use of Laboratory Animals by the US National Institutes of Health.

Statistical analysis

All statistical analyses were performed with GraphPad Prism 7.00 software (San Diego, CA, USA). Students' t-tests analyzed quantitative data. At least three samples were tested in each assay. All data are represented as the means ± SD, and a *p*-value < 0.05 was considered statistically significant.

Abbreviation

ICC, Intrahepatic Cholangiocarcinoma; TBK1, TANK-binding kinase 1; CCA, Cholangiocarcinoma; ECC, extrahepatic Cholangiocarcinoma; GO, Gene Ontology; GSEA, Gene Set Enrichment Analysis; TAA, thioacetamide; DEN, diethylnitrosamine; CCl_4, Carbon tetrachloride; EMT, epithelial-mesenchymal transition; OS, overall survival; DFS, disease-free survival; PDAC, pancreatic ductal adenocarcinoma; TNF, tumor necrosis factor.

Declarations

Acknowledgment

We thank the Central Laboratory, School of Medicine, Jinan University, for providing the facilities and assistance that supported this research.

Author Contributions

N.Y., K.C., and J.H. designed the study. J.H., Z.C., and C.G. wrote the manuscript. C.G., Y.X., J.W., Z.C., and X.Z. carried out the experiments. C.G., Z.C., Y.H., Y.J., and X.Z. performed data analysis. D.C., J.Z., and K.C. helped in experimental design and contributed materials. Y.X., X.Z., and J.W. helped in experimental design and writing. All authors have seen and approved the final version of the manuscript.

Compliance with ethical standards

Conflicts of Interest The authors disclose no conflicts.

Publisher's note

Springer Nature remains neutral with regard to jurisdictional claims in published maps and institutional affiliations.

Funding

National Natural Science Foundation of China (81871987 to JH; 8217100390 to NY; 82102782 to HY), Fundamental Research Funds for the Central Universities (21620106 to JH), and Science and Technology Program of Guangzhou, China (201904010001 to KC), Natural Science Foundation of Guangdong Province, China (2019A1515010145 to KC).

References

1. Siegel RL, Miller KD, Jemal A. Cancer statistics, 2020. CA: a cancer journal for clinicians. 2020;70(1):7–30.
2. Brindley PJ, Bachini M, Ilyas SI, Khan SA, Loukas A, Sirica AE, et al. Cholangiocarcinoma. Nature reviews Disease primers. 2021;7(1):65.
3. Banales JM, Cardinale V, Carpino G, Marzioni M, Andersen JB, Invernizzi P, et al. Expert consensus document: Cholangiocarcinoma: current knowledge and future perspectives consensus statement from the European Network for the Study of Cholangiocarcinoma (ENS-CCA). Nature reviews Gastroenterology & hepatology. 2016;13(5):261–80.
4. Banales JM, Marin JJG, Lamarca A, Rodrigues PM, Khan SA, Roberts LR, et al. Cholangiocarcinoma 2020: the next horizon in mechanisms and management. Nature reviews Gastroenterology & hepatology. 2020;17(9):557–88.
5. Kelley RK, Bridgewater J, Gores GJ, Zhu AX. Systemic therapies for intrahepatic cholangiocarcinoma. Journal of hepatology. 2020;72(2):353–63.
6. Cheng C, Ji Z, Sheng Y, Wang J, Sun Y, Zhao H, et al. Aphthous ulcer drug inhibits prostate tumor metastasis by targeting IKK□/TBK1/NF-κB signaling. Theranostics. 2018;8(17):4633–48.
7. Valle JW, Kelley RK, Nervi B, Oh DY, Zhu AX. Biliary tract cancer. Lancet (London, England). 2021;397(10272):428–44.
8. Abou-Alfa GK, Sahai V, Hollebecque A, Vaccaro G, Melisi D, Al-Rajabi R, et al. Pemigatinib for previously treated, locally advanced or metastatic cholangiocarcinoma: a multicentre, open-label, phase 2 study. The Lancet Oncology. 2020;21(5):671–84.
9. Kam AE, Masood A, Shroff RT. Current and emerging therapies for advanced biliary tract cancers. The lancet Gastroenterology & hepatology. 2021;6(11):956–69.
10. Qian Y, Yao W, Yang T, Yang Y, Liu Y, Shen Q, et al. aPKC-ι/P-Sp1/Snail signaling induces epithelial-mesenchymal transition and immunosuppression in cholangiocarcinoma. Hepatology (Baltimore, Md). 2017;66(4):1165–82.
11. Cruz VH, Arner EN, Du W, Bremauntz AE, Brekken RA. Axl-mediated activation of TBK1 drives epithelial plasticity in pancreatic cancer. JCI insight. 2019;5(9).

12. Affo S, Nair A, Brundu F, Ravichandra A, Bhattacharjee S, Matsuda M, et al. promotion of cholangiocarcinoma growth by diverse cancer-associated fibroblast subpopulations. Cancer cell. 2021;39(6):866 – 82.e11.
13. Recouvreux MV, Moldenhauer MR, Galenkamp KMO, Jung M, James B, Zhang Y, et al. Glutamine depletion regulates Slug to promote EMT and metastasis in pancreatic cancer. The Journal of experimental medicine. 2020;217(9).
14. Pastushenko I, Blanpain C. EMT Transition States during Tumor Progression and Metastasis. Trends in cell biology. 2019;29(3):212–26.
15. Bakir B, Chiarella AM, Pitarresi JR, Rustgi AK. EMT, MET, Plasticity, and Tumor Metastasis. Trends in cell biology. 2020;30(10):764–76.
16. Sawanyawisuth K, Sashida G, Sheng G. Epithelial-Mesenchymal Transition in Liver Fluke-Induced Cholangiocarcinoma. Cancers. 2021;13(4).
17. Liang S, Guo H, Ma K, Li X, Wu D, Wang Y, et al. A PLCB1-PI3K-AKT Signaling Axis Activates EMT to Promote Cholangiocarcinoma Progression. Cancer research. 2021;81(23):5889–903.
18. Yuan K, Xie K, Lan T, Xu L, Chen X, Li X, et al. TXNDC12 promotes EMT and metastasis of hepatocellular carcinoma cells via activation of β-catenin. Cell death and differentiation. 2020;27(4):1355–68.
19. Wen J, Min X, Shen M, Hua Q, Han Y, Zhao L, et al. ACLY facilitates colon cancer cell metastasis by CTNNB1. Journal of experimental & clinical cancer research: CR. 2019;38(1):401.
20. Xiang S, Song S, Tang H, Smaill JB, Wang A, Xie H, et al. TANK-binding kinase 1 (TBK1): An emerging therapeutic target for drug discovery. Drug discovery today. 2021;26(10):2445–55.
21. Jiang Y, Chen S, Li Q, Liang J, Lin W, Li J, et al. TANK-Binding Kinase 1 (TBK1) Serves as a Potential Target for Hepatocellular Carcinoma by Enhancing Tumor Immune Infiltration. Frontiers in immunology. 2021;12:612139.
22. Cruz VH, Brekken RA. Assessment of TANK-binding kinase 1 as a therapeutic target in cancer. Journal of cell communication and signaling. 2018;12(1):83–90.
23. Kawasaki K, Kuboki S, Furukawa K, Takayashiki T, Takano S, Ohtsuka M. LGR5 induces β-catenin activation and augments tumour progression by activating STAT3 in human intrahepatic cholangiocarcinoma. Liver international: official journal of the International Association for the Study of the Liver. 2021;41(4):865–81.
24. Shen W, Zhang X, Tang J, Zhang Z, Du R, Luo D, et al. CCL16 maintains stem cell-like properties in breast cancer by activating CCR2/GSK3β/β-catenin/OCT4 axis. Theranostics. 2021;11(5):2297–317.
25. Yeh HW, Hsu EC, Lee SS, Lang YD, Lin YC, Chang CY, et al. PSPC1 mediates TGF-β1 autocrine signalling and Smad2/3 target switching to promote EMT, stemness and metastasis. Nature cell biology. 2018;20(4):479–91.
26. Borhani S, Corciulo C, Larranaga-Vera A, Cronstein BN. Adenosine A(2A) receptor (A2AR) activation triggers Akt signaling and enhances nuclear localization of β-catenin in osteoblasts. FASEB journal:

official publication of the Federation of American Societies for Experimental Biology. 2019;33(6):7555–62.

27. Yao W, Cao Q, Luo S, He L, Yang C, Chen J, et al. Microglial ERK-NRBP1-CREB-BDNF signaling in sustained antidepressant actions of (R)-ketamine. Molecular psychiatry. 2022;27(3):1618–29.
28. Ohyagi M, Nagata T, Ihara K, Yoshida-Tanaka K, Nishi R, Miyata H, et al. DNA/RNA heteroduplex oligonucleotide technology for regulating lymphocytes in vivo. Nature communications. 2021;12(1):7344.
29. Zhang XF, Xue F, Dong DH, Weiss M, Popescu I, Marques HP, et al. Number and Station of Lymph Node Metastasis After Curative-intent Resection of Intrahepatic Cholangiocarcinoma Impact Prognosis. Annals of surgery. 2021;274(6):e1187-e95.
30. Park DD, Phoomak C, Xu G, Olney LP, Tran KA, Park SS, et al. metastasis of cholangiocarcinoma is promoted by extended high-mannose glycans. Proceedings of the National Academy of Sciences of the United States of America. 2020;117(14):7633–44.
31. Deng X, Jiang P, Chen J, Li J, Li D, He Y, et al. GATA6 promotes epithelial-mesenchymal transition and metastasis through MUC1/β-catenin pathway in cholangiocarcinoma. Cell death & disease. 2020;11(10):860.
32. Yang S, Liu Y, Li MY, Ng CSH, Yang SL, Wang S, et al. FOXP3 promotes tumor growth and metastasis by activating Wnt/β-catenin signaling pathway and EMT in non-small cell lung cancer. Molecular cancer. 2017;16(1):124.
33. Zhang Y, Unnithan RVM, Hamidi A, Caja L, Saupe F, Moustakas A, et al. TANK-binding kinase 1 is a mediator of platelet-induced EMT in mammary carcinoma cells. FASEB journal: official publication of the Federation of American Societies for Experimental Biology. 2019;33(7):7822–32.
34. Zhu L, Li Y, Xie X, Zhou X, Gu M, Jie Z, et al. TBKBP1 and TBK1 form a growth factor signalling axis mediating immunosuppression and tumourigenesis. Nature cell biology. 2019;21(12):1604–14.
35. Hu L, Xie H, Liu X, Potjewyd F, James LI, Wilkerson EM, et al. TBK1 Is a Synthetic Lethal Target in Cancer with VHL Loss. Cancer discovery. 2020;10(3):460–75.
36. Aiello NM, Kang Y. Context-dependent EMT programs in cancer metastasis. The Journal of experimental medicine. 2019;216(5):1016–26.
37. Zheng X, Carstens JL, Kim J, Scheible M, Kaye J, Sugimoto H, et al. Epithelial-to-mesenchymal transition is dispensable for metastasis but induces chemoresistance in pancreatic cancer. Nature. 2015;527(7579):525–30.
38. Wang W, Smits R, Hao H, He C. Wnt/β-Catenin Signaling in Liver Cancers. Cancers. 2019;11(7).
39. Edeline J, Touchefeu Y, Guiu B, Farge O, Tougeron D, Baumgaertner I, et al. Radioembolization Plus Chemotherapy for First-line Treatment of Locally Advanced Intrahepatic Cholangiocarcinoma: A Phase 2 Clinical Trial. JAMA oncology. 2020;6(1):51–9.
40. Salimon M, Prieux-Klotz C, Tougeron D, Hautefeuille V, Caulet M, Gournay J, et al. gemcitabine plus platinum-based chemotherapy for first-line treatment of hepatocholangiocarcinoma: an AGEO French multicentre retrospective study. British journal of cancer. 2018;118(3):325–30.

41. Nagata T, Dwyer CA, Yoshida-Tanaka K, Ihara K, Ohyagi M, Kaburagi H, et al. Cholesterol-functionalized DNA/RNA heteroduplexes cross the blood-brain barrier and knock down genes in the rodent CNS. Nature biotechnology. 2021;39(12):1529–36.
42. Yuan H, Lin Z, Liu Y, Jiang Y, Liu K, Tu M, et al. Intrahepatic cholangiocarcinoma induced M2-polarized tumor-associated macrophages facilitate tumor growth and invasiveness. Cancer cell international. 2020;20(1):586.
43. Tu M, He L, You Y, Li J, Yao N, Qu C, et al. EFTUD2 maintains the survival of tumor cells and promotes hepatocellular carcinoma progression via the activation of STAT3. Cell death & disease. 2020;11(10):830.

Figures

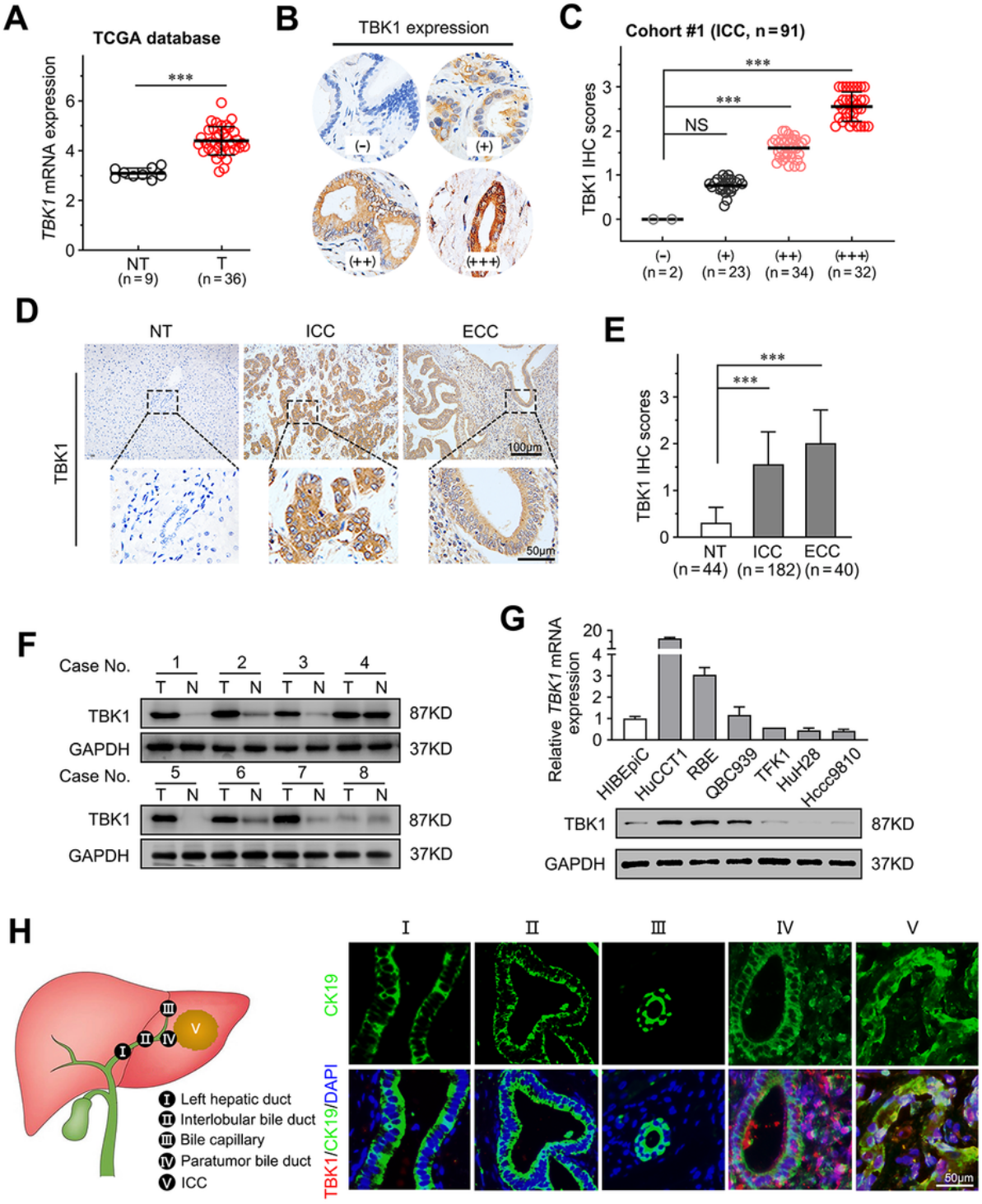

Figure 1

TANK-binding kinase 1 (TBK1) is upregulated in CCA. (A) The mRNA level of TBK1 expression among adjacent nontumor and ICC tissues (data from TCGA). **(B)** Representative images of IHC staining for TBK1 in cohort 1 (OUTDO Biotech, Shanghai, China, n = 91), including negative (−, 2.2%); weakly positive (+, 25.3%); moderately positive (++, 37.4%) and strongly positive (+++□35.1%). **(C)** Quantification of TBK1 expression in cohort 1. The data are the means ± SD. **(D)** Representative images of IHC staining for TBK1

in Our cohort, including normal hepatic (n = 44), ICC (n = 182) and ECC (n = 40). The scale bars are 100 μm (upper) and 50 μm (lower). **(E)** Quantification of TBK1 expression. The data are the means ± SD. **(F)** Western blot analysis of TBK1 expression in ICC tumor and paired adjacent nontumor tissues. T tumor tissue, N peritumoral normal tissues. **(G)** The mRNA and protein levels of TBK1 expression in CCA cells were detected by qPCR and western blot. **(H)** Representative immunofluorescence images of CK19 (green) and TBK1 (red) labeling in the same patient's normal, adjacent nontumor, and ICC tissues. Scale bar, 50 μm. ***$P < 0.001$.

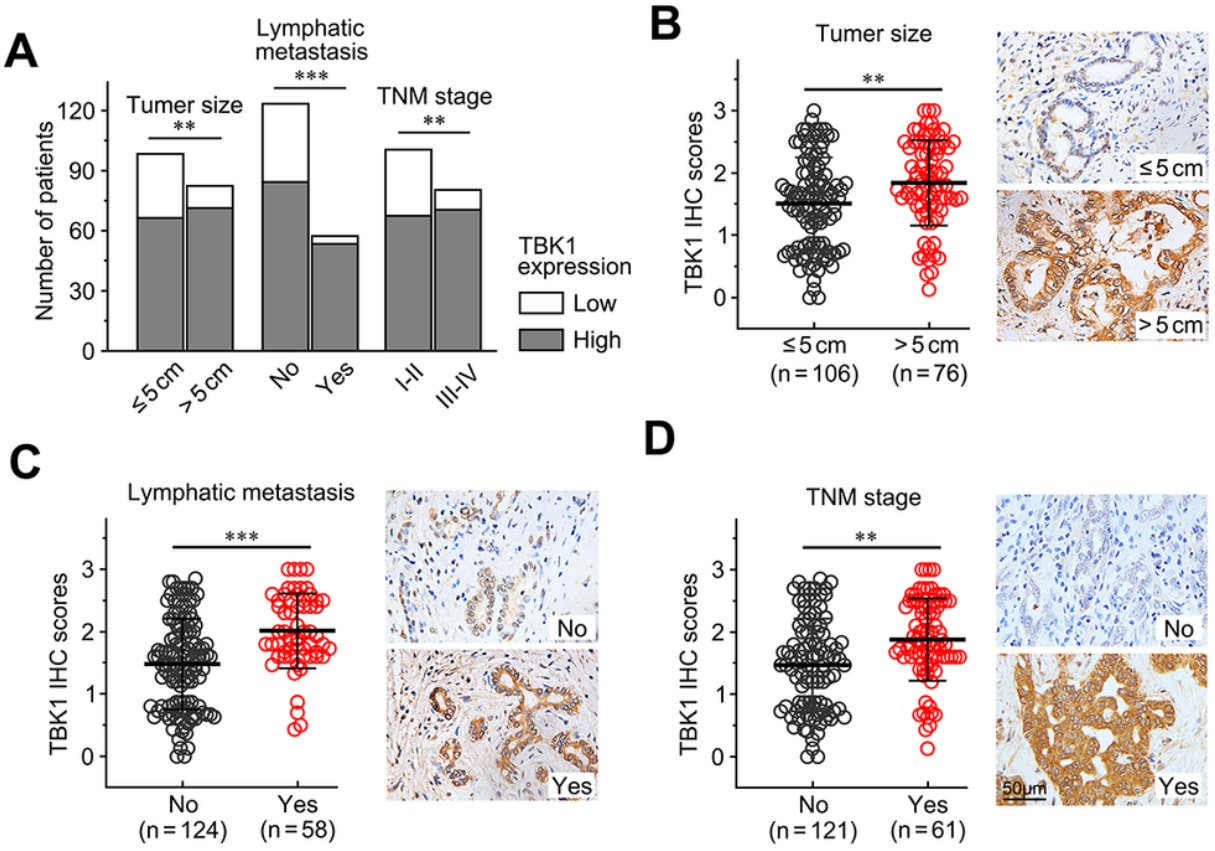

Figure 2

Correlation between TBK1 expression and clinicopathological factors. (A) The bar chart shows the positive correlation between TBK1 and larger tumor diameter, Lymph node metastasis, or advanced TNM stage. **(B)** The left panel shows the Quantification of TBK1 expression with different tumor sizes in our cohort (n = 182). The data are the means ± SD. The right panel shows the representative images of IHC staining for TBK1 in different tumor sizes. **(C)** The left panel shows the Quantification of TBK1 expression with Lymph node metastasis in our cohort (n = 182). The data are the means ± SD. The right

panel shows the representative images of IHC staining for TBK1 with or without Lymph node metastasis. **(D)** The left panel shows the quantification of TBK1 expression with advanced TNM stage in our cohort (n = 182). The data are the means ± SD. The right panel shows the representative images of IHC staining for TBK1 with or without Lymph node metastasis. ***P* < 0.01, ****P* < 0.001.

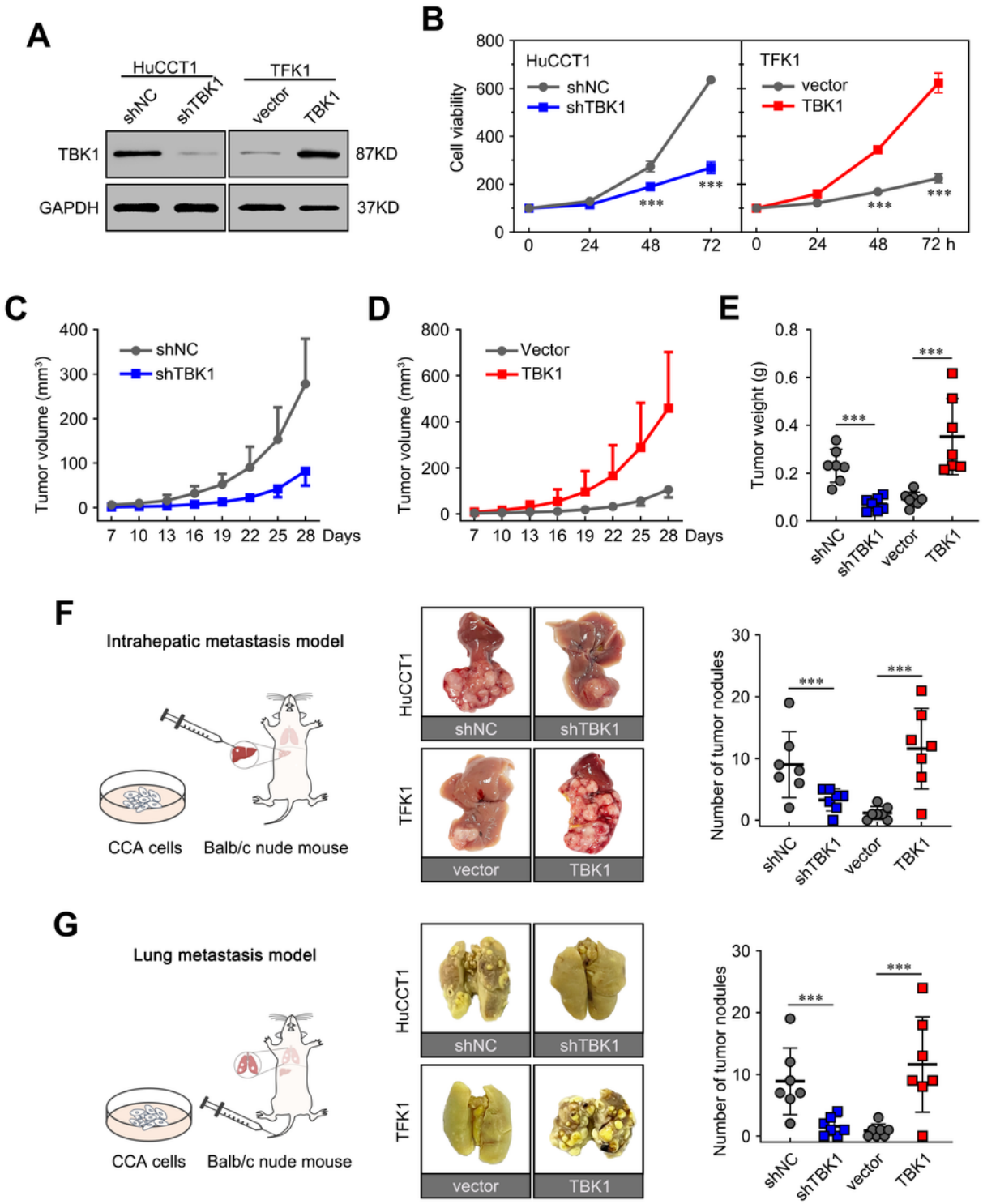

Figure 3

TBK1 promoted CCA cell growth, migration, and invasion both *in vitro* and *in vivo.*

(A) Knockout of TBK1 in HuCCT1 cells and overexpression of TBK1 in TFK1 cells, as confirmed by immunoblot analysis. **(B)** TBK1 stable depletion and overexpression effects on proliferation using Cell Counting Kit-8 assay. **(C, D)** TBK1 stable depletion and overexpression effects on the growth of *in vivo* subcutaneous xenograft tumors. Tumor size was monitored every three days, tumor volume: length × width² × 0.5. Tumor weight was recorded following harvesting. Results were presented as means ± SD. **(E)** The weight of subcutaneous tumors by injection of the indicated cells. **(F)** HuCCT1 and TFK1 cells infected with lentiviruses, as previously described, were inoculated orthotopically into the liver of 6-week-old male Balb/c nude mice (left), representative gross images (middle), and the quantification of liver metastasis nodules (right). Results were presented as means ± SD. (n = 7 per group). **(G)** HuCCT1 and TFK1 cells infected with lentiviruses, as previously described, were injected into mouse tail veins of 6-week-old male Balb/c nude mice (left) to construct a lung metastasis model representative gross images (middle) and the quantification of lung metastasis nodules (right). Results were presented as means ± SD. (n = 7 per group). ***$P < 0.001$.

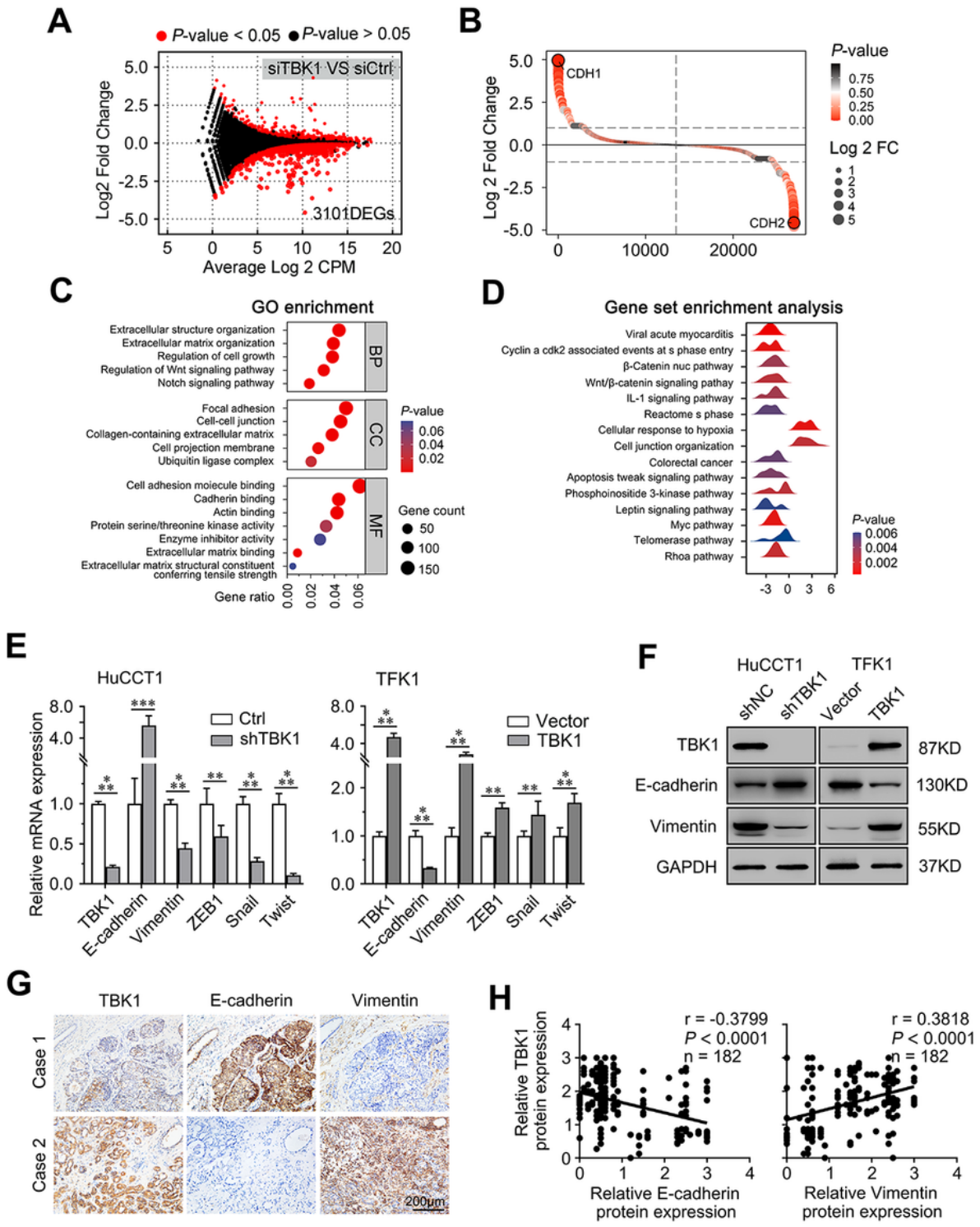

Figure 4

Upregulation of TBK1 promoted EMT in CCA. (A) Log ratio–average (M-A) plots showing the gene-expression changes in HuCCT1 cells afterTBK1 knockdown. **(B)** The significant upregulated or down-regulated genes in HuCCT1 cells after TBK1 knockdown was detected by RNA sequencing. **(C)** GO enrichment analysis of the DEGs. **(D)** Ridgeline plot depicting the significantly enriched signaling pathways of the DEGs revealed by GSEA. **(E)** Fold change in the mRNA levels of TBK1, E-cadherin,

Vimentin, ZEB1, Snail, and Twist in the TBK1 stable depletion and overexpression cells. The data are the means ± SD and represent three independent experiments. **(F)** The protein level of E-cadherin and Vimentin in the TBK1 stable depletion and overexpression cells was evaluated by western blotting. **(G)** Representative immunohistochemical staining of TBK1, E-cadherin, and Vimentin in human CCA tissues. scale bar = 200 μm. **(H)** Correlation analysis between TBK1 and E-cadherin, Vimentin expression in liver tumor tissues from patients with ICC (n = 182). $^{**}P < 0.01$, $^{***}P < 0.001$.

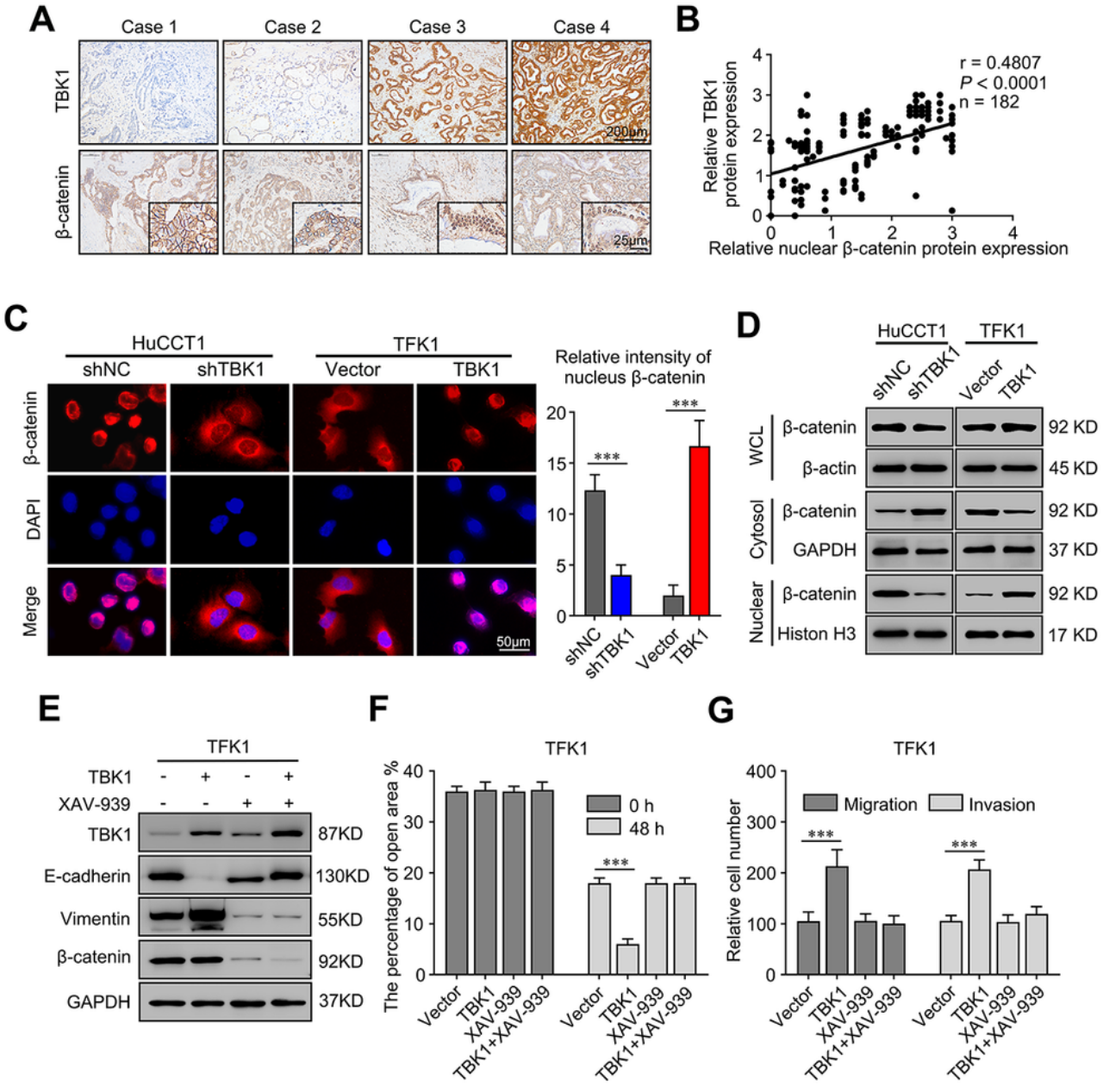

Figure 5

TBK1 promotes the EMT process through β-catenin activation. (A) Representative immunohistochemical staining of TBK1 and β-catenin in human ICC tissues. The scale bars are 200 μm (upper) and 25 μm (lower). **(B)** Correlation analysis between TBK1 and nuclear β-catenin expression in ICC tumor tissues from 182 patients. **(C)** β-Catenin expression in the indicated cells, as detected by an immunofluorescence assay. The merged images show overlays of β-catenin (red) and nuclear staining by DAPI (blue); scale bar: 50 μm. **(D)** β-Catenin expression in whole-cell lysates and the cytoplasmic, and nuclear fractions, as detected by immunoblot analysis. **(E)** Relative expression levels of TBK1, E-cadherin, Vimentin, and β-catenin in the indicated cells treated with or without XAV-939, a potent tankyrase inhibitor that inhibited nuclear entry of β-catenin. **(F)** Wound healing migration assays were performed with the indicated CCA cells treated with or without XAV-939. The data are the means ± SDs and represent three independent experiments. **(G)** Transwell migration and Matrigel invasion assays were performed with the indicated CCA cells treated with or without XAV-939. The data are the means ± SDs and represent three independent experiments. ***$P < 0.001$.

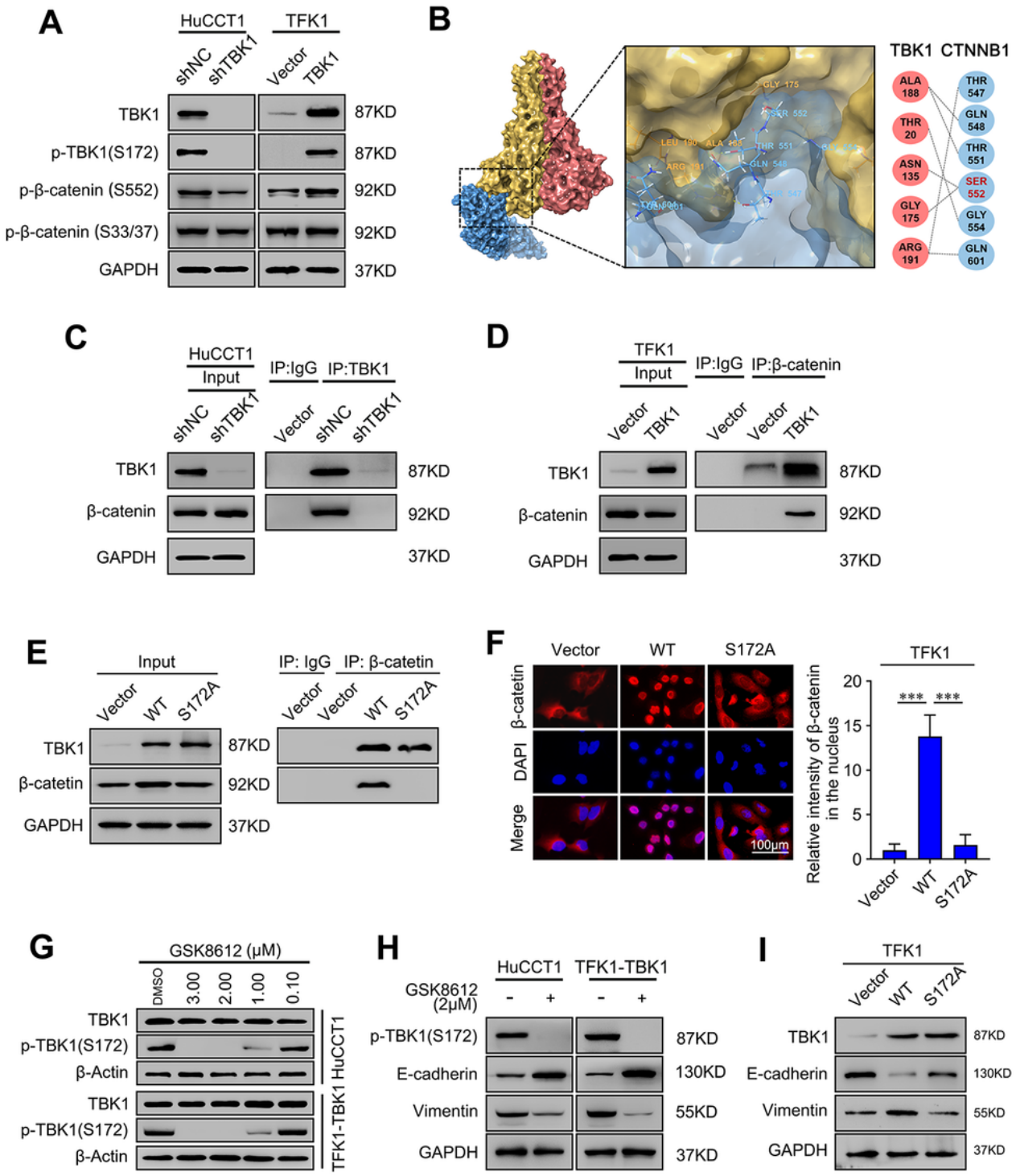

Figure 6

TBK1 activated β-catenin through direct interaction. (A) Western blot analysis of the expression of TBK1, p-TBK1, p-β-catenin (S552), and p-β-catenin (S33/37) proteins in indicated CCA cells. **(B)** Molecular docking model of TBK1 with β-catenin**. (C, D)** Immunoprecipitation of TBK1 with β-catenin in the indicated CCA cells, as detected by immunoblot analysis. **(E)** 293T cells transfected with Flag-tagged vector, wild-type TBK1 (WT), or Serine-mutated TBK1 (S172A) were immunoprecipitated with an anti-

TBK1 antibody. The β-catenin and TBK1 levels are indicated. **(F)** β-Catenin expression in the indicated cells, as detected by immunofluorescence assay. The merged images show overlays of β-catenin (red) and nuclear staining by DAPI (blue). scale bar = 100 mm. **(G)** Immunoblots of indicated proteins in HuCCT1 and TFK1 cells treated with different concentrations of GSK8612. **(H)** There are relative expression levels of p-TBK1, E-cadherin, and Vimentin in indicated cells treated with or without GSK8612 (2.0 μM). **(I)** Relative expression levels of TBK1, E-cadherin, and Vimentin in the indicated cells. ***$P <$ 0.001.

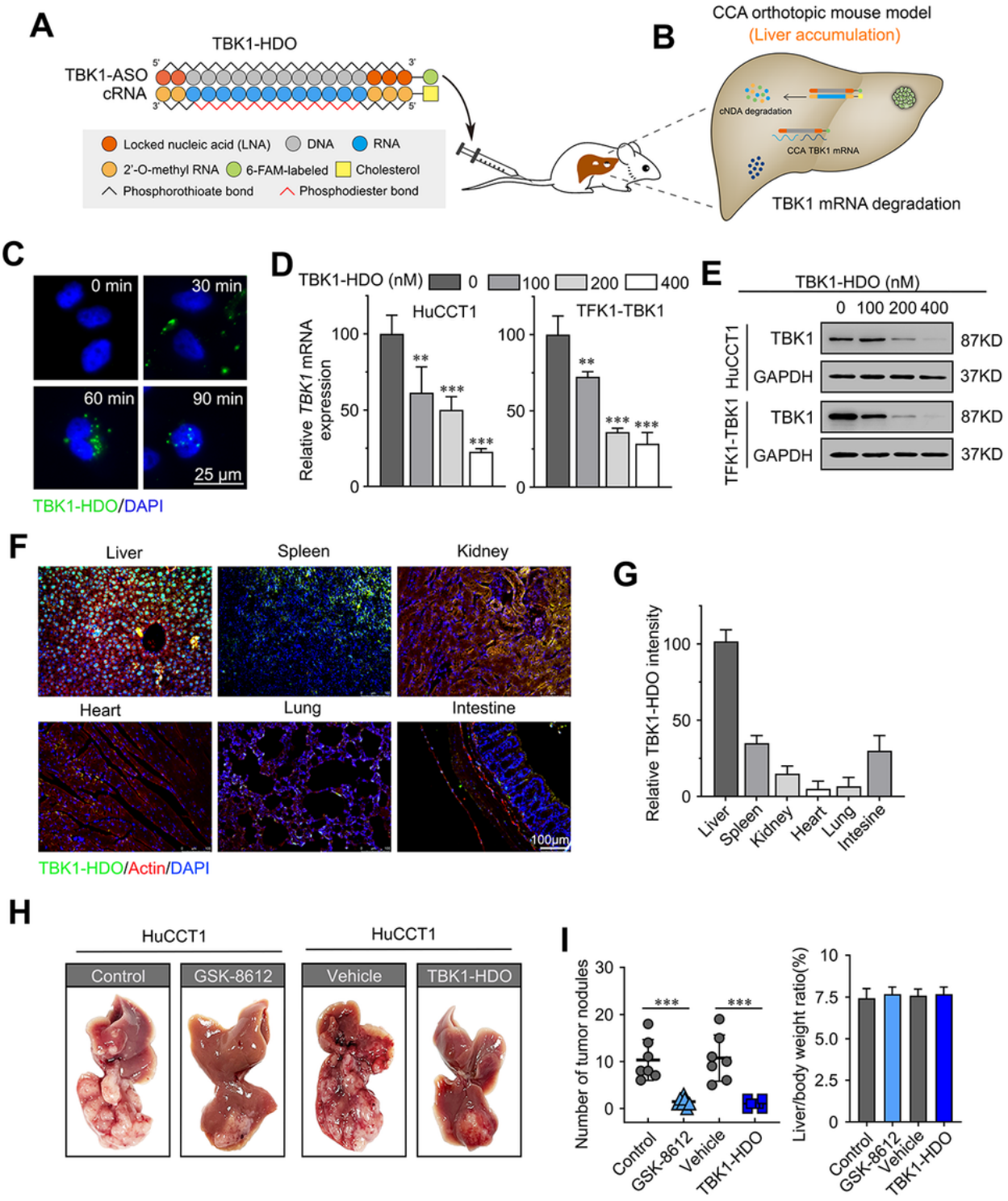

Figure 7

TBK1-HDO and Pharmacological inhibition of TBK1 reduce CCA cell growth *in vitro* and *in vivo.* (A) Schematic illustration of the construction of HDO and HDO targeting mouse TBK1 mRNA. **(B)** HDO is specifically concentrated in the liver and illustrates TBK1 degradation. **(C)** HuCCT1 and TFK1-TBK1 cells were treated with TBK1-HDO after 30 min, 60 min, and 90 min by immunofluorescence assay. Merged images represent overlays of TBK1-HDO (green) and nuclear staining by DAPI (blue). Scale bar = 25 μm. **(D, E)** Dose-dependent reduction of gene silencing in HuCCT1 and TFK1-TBK1 cells with HDO targeting TBK1. Data are representative of at least three independent experiments each. **(F)** Fluorescence micrographs of various mice organs 6 h after injection of 0.75 mg/kg 6-FAM-labeled TBK1-HDO. Green: 6-FAM-labeled DNA/LNA gapmer; Red: Actin; Blue: DAPI. Scale bar = 100 μm. **(G)** The quantification of TBK1-HDO expression in various mice organs. **(H, I)** Statistical analysis of tumor nodules and the liver/body weight ratio, as well as representative images of tumor morphology of liver tissue *in vivo* at the endpoint.

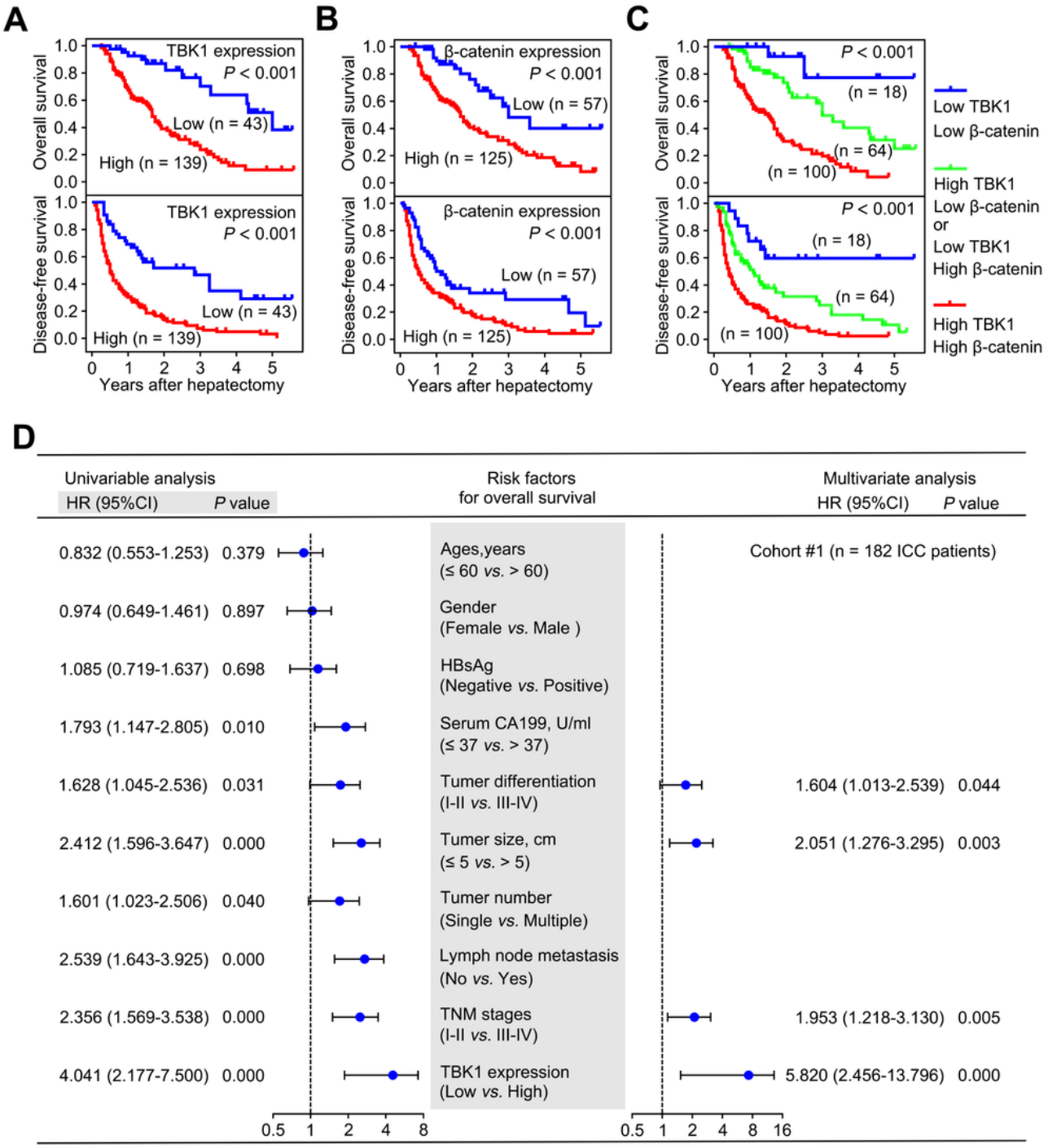

Figure 8

Upregulation of TBK1 predicts poor survival in ICC patients. (A) Overall survival (OS) and disease-free survival (DFS) curves of patients from the First Affiliated Hospital, Sun Yat□sen University dataset (our cohort, n=182) with high or low TBK1 expression levels. **(B)** Overall survival (OS) and disease-free survival (DFS) curves of patients from the First Affiliated Hospital, Sun Yat□sen University dataset (our cohort, n=182) with high or low β-catenin expression levels. **(C)** OS and DFS curves are stratified by TBK1 and

nuclear β-catenin expression levels. ICC patients were classified into three groups according to TBK1 and nuclear β-catenin expression: group1 (n = 18): low TBK1 and β-catenin expression; group2 (n = 64): high TBK1 and low β-catenin expression or low TBK1 and high β-catenin expression; group3 (n = 100): high TBK1 and β-catenin expression. **(D)** Univariate and multivariate analyses of factors possibly associated with overall and disease-free survival after resection in our cohort (n = 182). ***P* < 0.01, ****P* < 0.001.

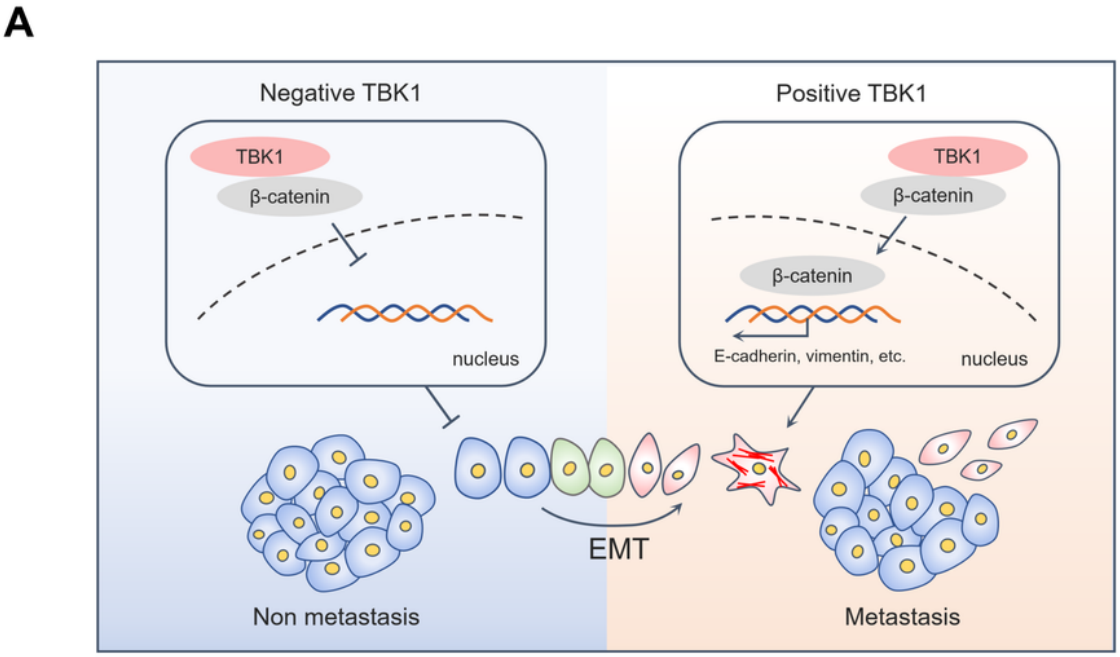

Figure 9

Legend not included with this version

Supplementary Files

This is a list of supplementary files associated with this preprint. Click to download.

- SupplementalMaterial1.doc
- SupplementalMaterial2.doc
- SupplementaryFig.1.tif
- SupplementaryFig.2.tif
- SupplementaryFig.3.tif
- SupplementaryFig.4.tif
- SupplementaryFig.5.tif
- SupplementaryFig.6.tif
- SupplementaryFig.7.tif
- SupplementaryFig.8.tif
- SupplementaryFig.9.tif
- SupplementaryFig.10.tif
- SupplementaryTable1.doc
- SupplementaryTable2.doc
- SupplementaryTable3.doc
- SupplementaryTable4.doc
- SupplementaryTable5.doc